

species in solution of **6a**, while the *gem* isomer is found exclusively in the solid state.

Acknowledgment. This research was supported in part by National Science Foundation Grant CHE-84-05517. Z.X. thanks Alpha Association of Phi Beta Kappa Alumni for a Graduate Scholarship.

Supplementary Material Available: Synthesis of $(C_6H_5)_3C\equiv$

$^*C(C_6H_5)$, a detailed description of the crystallographic studies and the programs used in data refinement, packing diagrams of **5b** (Figure A) and **6a** (Figure B), $^{13}C\{^1H\}$ NMR spectra of the carbonyl region for **3** and **4** (Figure C), final atomic parameters for **5b** (Table A) and **6a** (Table B), final thermal parameters for **5b** (Table C) and **6a** (Table D), comparison of ^{13}C chemical shifts in σ - and σ,π -vinyl derivatives (Table E) (18 pages); tables of observed and calculated structure factors for **5b** and **6a** (47 pages). Ordering information is given on any current masthead page.

Reactions of Primary and Secondary Silanes with Binuclear Rhodium Complexes. Formation of μ -Silylene Complexes and P-Si Bonds with Facile P-C Bond Cleavage

Wei-Dong Wang and Richard Eisenberg*

Contribution from the Department of Chemistry, University of Rochester, Rochester, New York 14627. Received June 27, 1989

Abstract: A series of bis(μ -SiRH) complexes $Rh_2(\mu-SiRH)_2(CO)_2(dpEm)_2$ (E = P: **3a**, R = Ph; **3b**, R = Et; **3c**, R = *n*-C₆H₁₃; and E = As: **6a**, R = Ph; **6b**, R = Et; **6c**, R = *n*-C₆H₁₃) has been synthesized from the reaction of the corresponding primary silane RSiH₃ and $Rh_2(\mu-H)_2(CO)_2(dpEm)_2$ (**1**, E = P; **4**, E = As). The bis μ -SiRH complexes **3** and **6** are characterized by 1H and $^{31}P\{^1H\}$ NMR and IR spectroscopies and for the Et and Ph derivatives, **3b** and **3a**, respectively, by X-ray crystallography. Crystallographic data for **3b**: C2/c; *a* = 24.184 (5) Å, *b* = 9.948 (3) Å, *c* = 24.059 (5) Å; β = 114.49 (2)°; *Z* = 4; d_{calcd} = 1.45 g/cm³; *R* = 0.034, *R*_w = 0.045. The structure determination of **3b** shows it to be a "cradle-like" structure with a Rh-Rh bond of 2.814 (1) Å and bridging SiEtH ligands. Each Rh center possesses an approximately square pyramidal coordination geometry ignoring the stereochemical influence of the Rh-Rh bond. In the reaction of **1** with RSiH₃, an intermediate has been identified as $Rh_2(\mu-SiRH)(H)_2(CO)_2(dppm)_2$ (**2a**, R = Ph; **2b**, R = Et; **2c**, R = *n*-C₆H₁₃) on the basis of spectroscopic data. This intermediate is fluxional with exchange occurring between Si-H and Rh-H protons, presumably by facile reductive elimination/oxidative addition of Si-H bonds to the Rh centers. For the dpam system **4**, different intermediates of the type $Rh_2(\mu-SiRH)(SiRH_2)(H)_3(CO)_2(dpam)_2$ (**5a**, R = Ph; **5b**, R = Et; **5c**, R = *n*-C₆H₁₃) are observed in the reaction with RSiH₃. Secondary silanes RR'SiH₂ react with **1** to produce initially the μ -SiRR' dihydride intermediates $Rh_2(\mu-SiRR')(H)_2(CO)_2(dppm)_2$ (**9a**, R = R' = Me; **9b**, R = R' = Et; **9c**, R = Me, R' = Ph) but ultimately give a new type of complex in which P-C cleavage and P-Si bond formation have occurred. These complexes are of the formula $Rh_2(\mu-H)(CO)_2(dppm)(Ph_2PCH_2PPhSiRR')$ (**10a**, R = R' = Me; **10b**, R = R' = Et; **10c**, R = Me, R' = Ph) and have been characterized by 1H and $^{31}P\{^1H\}$ NMR and IR spectroscopies, and for **10b** by X-ray crystallography. X-ray data for **10b**: P2₁; *a* = 11.387 (2) Å, *b* = 18.959 (3) Å, *c* = 13.354 (2) Å; β = 112.50 (1)°; *Z* = 2; d_{calcd} = 1.30 g/cm³; *R* = 0.029, *R*_w = 0.041. In a related reaction, the tricarbonyl complex $Rh_2(CO)_3(dppm)_2$ (**7**) reacts with RSiH₃ leading initially to the formation of **2** followed by conversion to the μ -CO complex $Rh_2(\mu-SiRH)(\mu-CO)(CO)_2(dppm)_2$ (**8**) which can also form by placing a solution of **2** under CO.

The reaction chemistry between silanes and complexes of the platinum group elements is exceedingly rich and involves Si-H oxidative addition,¹ hydrosilation catalysis,² redistribution reactions,³ and most recently metal complex promoted oligomerization of silanes.⁴⁻⁹ This last reaction is of special interest because it

addresses a basic chemical question of coupling saturated silyl moieties and provides a potential entry into a new method for preparing silane oligomers and polymers. These materials, and in particular the polysilanes, are under active study because of their properties as materials and material precursors, but the process of synthesizing them still relies on Wurtz-type coupling reactions with silyl chlorides and active metals.¹⁰

Recently other approaches to forming Si-Si bonds based on transition-metal catalysis have been explored for the generation of polysilanes. These approaches with primary and secondary silanes, R_nSiH_{4-n} (*n* = 1, 2; R = alkyl, aryl), as starting materials have been termed *dehydrogenative coupling* and occur with concomitant evolution of H₂. In 1985, Harrod and co-workers

(1) (a) MacKay, K. M.; Nicholson, B. K. In *Comprehensive Organometallics*; Wilkinson, G., Stone, F. G. A., Abel, E. W., Eds.; Pergamon: Oxford, 1982; Vol. 6, Chapter 43, p 1043. (b) Aylett, B. J. *Adv. Inorg. Radiochem.* **1982**, *25*, 1.

(2) Collman, J. P.; Hegedus, L. S.; Norton, J. R.; Finke, R. G. *Principles and Applications of Organotransition Metal Chemistry*; University Science Books: Mill Valley, CA, 1987; pp 293, 564, 761 and references therein.

(3) (a) Fernandez, M. L.; Maitlis, P. M. *J. Chem. Soc. Dalton Trans.* **1984**, 2063. (b) Curtis, M. D.; Epstein, P. S. *Adv. Organomet. Chem.* **1981**, *19*, 213.

(4) (a) Aitken, C. T.; Harrod, J. F.; Samuel, E. J. *Organomet. Chem.* **1985**, *279*, C11. (b) Harrod, J. F.; Aitken, C. T. International Chemical Congress of the Pacific Basin Societies, Honolulu, Hawaii, 1984; Paper 7K12.

(5) Aitken, C. T.; Harrod, J. F.; Samuel, E. J. *Am. Chem. Soc.* **1986**, *108*, 4059.

(6) Ojima, I.; Inaba, S. I.; Kogure, T.; Nagai, Y. *J. Organomet. Chem.* **1973**, *55*, C7.

(7) (a) Corey, J. Y.; Chang, L. S.; Corey, E. R. *Organometallics* **1987**, *6*, 1595. (b) Brown-Wensley, K. A. *Organometallics* **1987**, *6*, 1590.

(8) Zarate, E. A.; Tessier-Youngs, C. A.; Youngs, W. J. *J. Am. Chem. Soc.* **1988**, *110*, 4068.

(9) (a) Woo, H. G.; Tilley, T. D. *J. Am. Chem. Soc.* **1989**, *111*, 3757. (b) Woo, H. G.; Tilley, T. D. *J. Am. Chem. Soc.* **1989**, *111*, 8043. (c) Tilley, T. D. Personal communication.

(10) West, R. In *Comprehensive Organometallics*; Wilkinson, G., Stone, F. G. A., Abel, E. W., Eds.; Pergamon: Oxford, 1982; Vol. 2, Chapter 9.4, p 365.

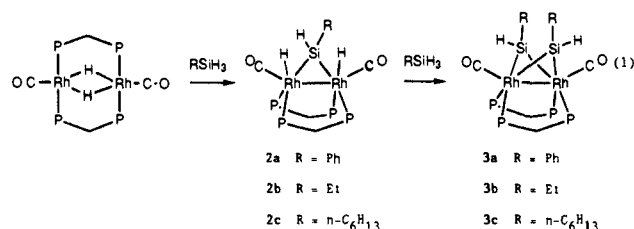
employed this approach with $\text{Cp}_2\text{TiR}'_2$ ($\text{R}' = \text{Me}, \text{CH}_2\text{Ph}$) as the catalyst to obtain $(\text{RSiH})_x$ with $x = \sim 10$.⁴ In the course of this work, they obtained binuclear intermediates having $\mu\text{-SiRH}_2$ groups ($\text{R} = \text{Ph}$) and observed Si-H/hydride exchange.⁵ Recently Tilley and Woo have proposed a mechanism for the dehydrogenative polymerization of silanes to polysilanes based on σ -bond metathesis.⁹ One of the key features of their proposed catalytic cycle is that coordinatively unsaturated metal hydrides serve as the active catalysts.^{9b}

The dehydrogenative coupling of silanes with complexes of the platinum group elements as catalysts has been reported within the last several years.⁶⁻⁸ However, in these studies the products were either Si-Si dimers or small oligomers with the formation of polymers remaining elusive. Of the catalyst systems surveyed, the complex $\text{RhCl}(\text{PPh}_3)_3$ was found to be most effective.^{7b} However, the very recent study by Youngs and Tessier-Youngs with $\text{PtCl}_2(\text{PEt}_3)_2$ as the catalyst has led to the structural characterization of binuclear silylene bridged systems, $\text{Pt}_2(\mu\text{-SiXPh})(\mu\text{-SiYPh})(\text{PEt}_3)_4$ ($\text{X} = \text{Y} = \text{H}, \text{Cl}; \text{X} = \text{H}, \text{Y} = \text{Cl}$), which were also found to promote the oligomerization reaction.⁸ Moreover, the Si...Si distances in these structures, 2.57–2.60 Å, were taken to suggest nascent Si-Si bond formation.

Our own work, which to date has not yielded Si-Si coupling, was stimulated by the striking similarity of H_2 and Si-H in oxidative addition reactions and by the reactivity of binuclear rhodium complexes containing bridging dppm ligands, which could lead to the simultaneous activation of more than one silane substrate. In this paper we describe in detail our studies, some of which have appeared in preliminary form.^{11a} Specifically, the reactions of primary and secondary silanes with the binuclear complexes $\text{Rh}_2\text{H}_2(\text{CO})_2(\text{dppm})_2$, $\text{Rh}_2(\text{CO})_3(\text{dppm})_2$, and $\text{Rh}_2\text{H}_2(\text{CO})_2(\text{dpam})_2$ (dppm = bis(diphenylphosphino)methane, dpam = bis(diphenylarsino)methane) leading to the formation of silylene-bridged complexes are reported, including the formation of $\mu\text{-SiRR}'$ hydride intermediates. For secondary silanes, a novel reaction is seen to occur in which a Si-P bond forms concomitant with P-C cleavage in the bridging dppm ligand.

Results and Discussion

Reactions of $\text{Rh}_2\text{H}_2(\text{CO})_2(\text{dppm})_2$ (1) with Primary Silanes, RSiH_3 . The reaction of 1 with RSiH_3 for $\text{R} = \text{Ph}$ and Et has been reported in preliminary form.^{11a} Completely analogous reaction chemistry occurs with $n\text{-C}_6\text{H}_{13}\text{SiH}_3$ as well. The reaction proceeds as in eq 1 with the initial formation of an intermediate $\mu\text{-SiRH}$ hydride species 2a-c and subsequent conversion to the bis($\mu\text{-SiRH}$) complex 3a-c. Both 2a-c and 3a-c have been characterized by ^1H and $^{31}\text{P}\{^1\text{H}\}$ NMR and IR spectroscopies. The structure of 3 has been established by single-crystal X-ray diffraction studies with the Ph derivative 3a reported previously^{11a} and the ethyl derivative 3b described below.

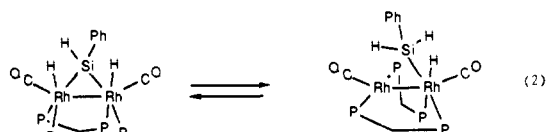


Species 2 is observed if the reaction is carried out at low temperatures (-30°C), and it can be isolated, although not analytically pure. Facile, subsequent reaction of 2 leading to the formation of 3 has precluded recrystallization and purification to date. A notable feature of 2 is that it is fluxional. At room temperature the ^1H NMR spectrum of the complex for $\text{R} = \text{Ph}$ (2a) reveals a broad resonance spanning 2 ppm at ca. -4.1 ppm and two dppm methylene resonances. Upon cooling, the former resonance resolves into two highly coupled patterns at $\delta -9.23$ and

6.33 ppm in a 2:1 intensity ratio assignable to Rh-H and Si-H resonances, respectively, while the dppm $-\text{CH}_2-$ protons split into four inequivalent signals. The $\delta -9.23$ ppm resonance shows the same second-order splitting pattern at both 400 and 500 MHz, and a satisfactory fit of this resonance at -70°C has been obtained assuming an AA'MM'XX' pattern with the following parameters: $J_{AA'} = 5$ Hz, $J_{AM} = J_{AM'} = 143$ Hz, $J_{AX} = J_{AX'} = 21.7$ Hz, $J_{AM'} = J_{A'M} = 14$ Hz, $J_{AX'} = J_{A'X} = -8.6$ Hz, $J_{MM'} = 144$ Hz, $J_{MX} = J_{M'X'} = 93$ Hz, $J_{M'X} = J_{MX'} = -24$ Hz, $J_{XX'} = 61$ Hz. Significantly, the fit contains only one large J_{HP} . Species 2b and 2c behave similarly, and the variable-temperature ^1H NMR spectrum of 2c is shown in Figure 1.

The $^{31}\text{P}\{^1\text{H}\}$ NMR spectra of 2a-c exhibit resonances due to two inequivalent sets of phosphine donors, and for 2a and 2b, the hydride-coupled spectra reveal that in each case only one of the two sets has significant phosphorus-hydride coupling. From these results and other spectroscopic characterization, species 2a-c is formulated as the μ -alkylsilylene hydride $\text{Rh}_2\text{H}_2(\mu\text{-SiRH})(\text{CO})_2(\text{dppm})_2$ with the structure as shown in eq 1. This structure is consistent with the one large hydride-phosphorus coupling observed experimentally and with the crystallographically determined structures of 3a and 3b (vide infra). Cowie has very recently determined the crystal structure of an iridium analogue of 2 and it agrees completely with the structure shown above.^{11bc}

The fluxionality of 2a-c involves exchange of the hydrogen atoms bound to rhodium and silicon. If the basic "cradle" structure with cis dppm ligands is preserved throughout the exchange, then the dppm $-\text{CH}_2-$ protons should coalesce from four resonances into two as is readily seen. From the coalescence temperatures of the two sets of dppm methylene protons and the Rh-H/Si-H exchange, ΔG^\ddagger for the process is calculated to be 12 ± 1 kcal/mol at both -30 and 25°C for 2a and 11 ± 1 kcal/mol at both -50 and 12°C for 2b, indicating a very small ΔS^\ddagger for the fluxional process. On the basis of the reactivity of Si-H bonds with Rh(I) centers, we propose that the fluxionality of 2a-c is due to rapid reductive elimination and oxidative addition of Si-H bonds via a $\text{Rh}_2\text{H}(\text{SiH}_2\text{R})(\text{CO})_2(\text{dppm})_2$ intermediate as in eq 2. Harrod



et al. have observed a similar exchange, but in their case the equilibration was between $\mu\text{-SiPhH}_2$ and $\mu\text{-H}$ hydrogen atoms of $\text{Cp}_2\text{Ti}(\mu\text{-H})(\mu\text{-SiPhH}_2)\text{TiCp}_2$.⁵ The mechanism for the latter exchange may be different from that shown in eq 2.

The bis($\mu\text{-SiRH}$) product 3a-c of eq 1 forms upon heating or prolonged reaction time. It is stable and isolable in pure form for the three primary silanes employed. Spectroscopic data are consistent with the structure determined crystallographically. The structure of the Ph derivative, 3a, has been reported previously and that of the Et derivative, 3b, is described immediately below. In the ^1H NMR spectra of 3b and 3c, the SiH resonances show coupling to the $\alpha\text{-CH}_2$ protons of the alkyl group.

The Molecular Structure of the Bis($\mu\text{-SiEtH}$) Product, 3b. Crystal data, data collection, and refinement parameters for the structure determination of 3b are summarized in Table I. Selected bond distances and angles are tabulated in Table II. The molecular structure of 3b, which is very similar to that of 3a, is illustrated in Figure 2. The structure contains two bridging ethylsilylene units, each bonded to two Rh atoms with an average distance of 2.348 (2) Å. The two Rh atoms are also joined directly by a single bond of length 2.814 (1) Å as well as by bridging dppm ligands. The overall geometry of 3 is of the $\text{Co}_2(\mu\text{-RC}\equiv\text{CR})(\text{CO})_6$ -type assuming two coordination sites for the $\mu\text{-RC}\equiv\text{CR}$ ligand¹² and is structurally very similar to the "cradle" complexes $\text{Rh}_2(\mu\text{-PhC}\equiv\text{CPh})(\text{CO})_2(\text{dppm})_2$ ¹³ and $\text{Ir}_2(\mu\text{-RNC})_2(\text{RNC})_2$

(11) (a) Wang, W. D.; Hommeltoft, S. I.; Eisenberg, R. *Organometallics* 1988, 7, 2417. (b) Cowie, M. Personal communication. (c) McDonald, R.; Cowie, M. Canadian Chemical Conference, Victoria, B.C., June 1989.

(12) (a) Hoffman, D. W.; Hoffman, R.; Fisel, C. R. *J. Am. Chem. Soc.* 1982, 104, 3858–3875. (b) Dickson, R. S.; Fraser, P. J. *Adv. Organomet. Chem.* 1974, 12, 323–377.

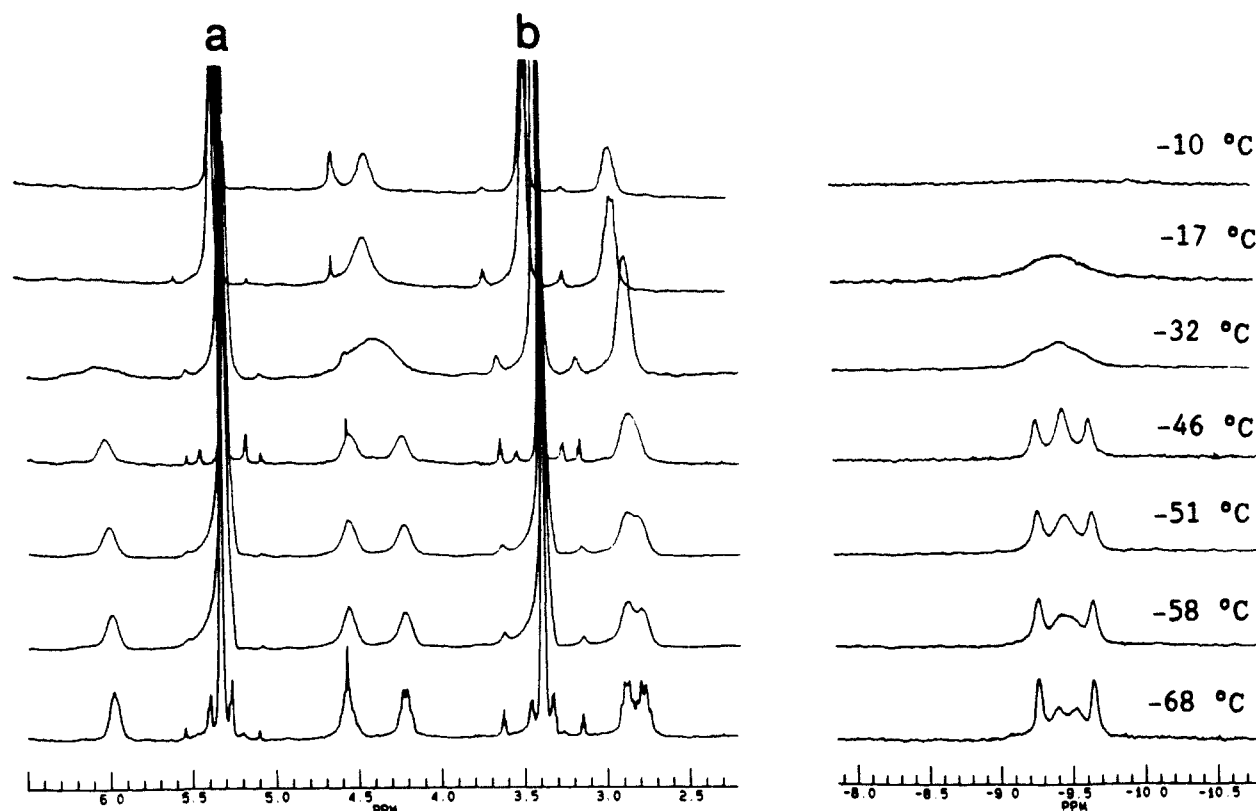


Figure 1. Variable-temperature ^1H NMR spectra of **2c** in CD_2Cl_2 . The resonances marked a and b correspond to CHDCl_2 and free $n\text{-C}_6\text{H}_{13}\text{SiH}_3$, respectively.

Table I. Summary of Crystal Data and Data Collection and Refinement Parameters^a

	3b	10b
formula	$\text{Rh}_2\text{P}_4\text{Si}_2\text{O}_2\text{C}_{56}\text{H}_{56}$	$\text{Rh}_2\text{P}_4\text{Si}_2\text{O}_2\text{C}_{50}\text{H}_{50}$
formula wt	1146.93	1040.69
crystal system	monoclinic	monoclinic
space group	$C2/c$	$P2_1$
<i>a</i> , Å	24.184 (5)	11.387 (2)
<i>b</i> , Å	9.948 (3)	18.959 (3)
<i>c</i> , Å	24.059 (5)	13.354 (2)
β , deg	114.49 (2)	112.50 (1)
<i>V</i> , Å ³	5268	2664
<i>Z</i>	4	2
<i>d</i> _{calc} , g/cm ³	1.45	1.30
radiation (Mo $K\alpha$), Å	0.71069	0.71069
$\mu(\text{Mo } K\alpha)$, cm ⁻¹	7.85	7.85
<i>T</i> , °C	23	23
trans coeff	0.740–1.214	0.867–1.129
total reflcns measured	3319	2847
no. of independent observatns	1978	2400
(<i>I</i> > 3 σ (<i>I</i>))		
no. of variables refined	298	555
<i>R</i>	0.034	0.029
<i>R</i> _w	0.045	0.041

^aCalculations were carried out with the Enraf-Nonius CAD4 and SDP-Plus programs. The function minimized in the least-squares refinements was $\sum w(|F_o| - |F_c|)^2$ where $w = 1/\sigma(F_o)^2$. The residuals are defined as $R = \sum (||F_o| - |F_c||) / \sum |F_o|$ and $R_w = \{\sum w(|F_o| - |F_c|)^2 / \sum w(F_o)^2\}^{1/2}$. The goodness of fit or the error in an observation of unit weight is defined as $\{\sum w(|F_o| - |F_c|)^2 / (\text{NO} - \text{NV})\}^{1/2}$ where NO is the number of observations and NV is the number of variables.

(dppm)₂ where R = 2,6-xylyl.¹⁴

The Si...Si separation in **3b** is 2.85 Å as compared with 2.75 Å in the structure of **3a**. These values, while longer than a Si-Si single bond, are substantially shorter than a van der Waal's

Table II. Selected Bond Distances (Å) and Angles (deg) for $\text{Rh}_2(\mu\text{-SiEtH}_2)(\text{CO})_2(\text{dppm})_2$ (**3b**)

Rh1-Rh2	2.814 (1)	Si1-C3	1.867 (8)	Rh1-P2	2.367 (2)
Rh2-Si1	2.354 (2)	C1-O1	1.146 (8)	C3-C4	1.52 (1)
Rh1-P1	2.363 (2)	Rh1-Si1	2.342 (2)	P1-C11	1.822 (7)
		Rh1-Cl1	1.868 (8)		
P1-Rh1-Si1	82.86 (7)	P2-Rh1-Si1	147.64 (6)		
Si1-Rh1-Si2	74.7 (1)	Rh1-Si1-Rh2	73.62 (6)		
Si1-Rh1-Rh2	53.38 (5)	C4-C3-Si1	114.8 (6)		
C3-Si1-Rh1	128.2 (3)	C3-Si1-Rh2	129.9 (3)		
C1-Rh1-Si1	103.4 (2)	C1-Rh1-Si2	103.7 (2)		
C1-Rh1-P1	104.7 (2)	C1-Rh1-P2	105.7 (2)		
O1-C1-Rh1	178.9 (7)	C1-Rh1-Rh2	148.2 (2)		

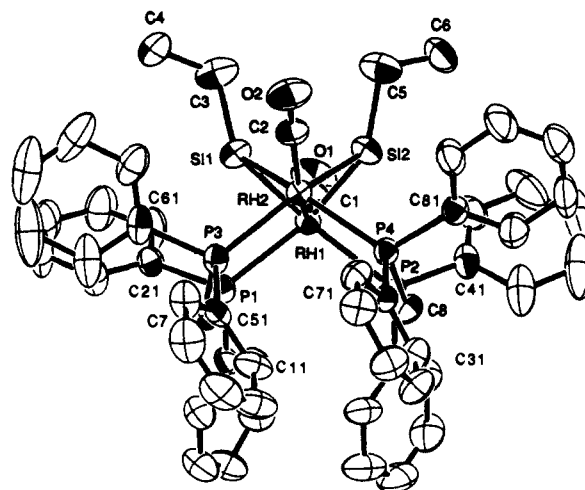


Figure 2. ORTEP drawing of $\text{Rh}_2(\text{SiEtH}_2)(\text{CO})_2(\text{dppm})_2$ (**3b**).

contact. The observed values of 2.75 and 2.85 Å in **3a** and **3b** are closer to the 2.57–2.60 Å range found for $\text{Pt}_2(\mu\text{-SiXPh})(\mu\text{-SiYPh})(\text{PEt}_3)_4$, in which nascent Si...Si bond formation was proposed,⁸ than the 3.85–4.22 Å range calculated for other bis-

(13) Berry, D. H.; Eisenberg, R. *Organometallics* **1987**, *6*, 1796.

(14) Wu, J.; Fanwick, P. E.; Kubiak, C. P. *J. Am. Chem. Soc.* **1988**, *110*, 1319.

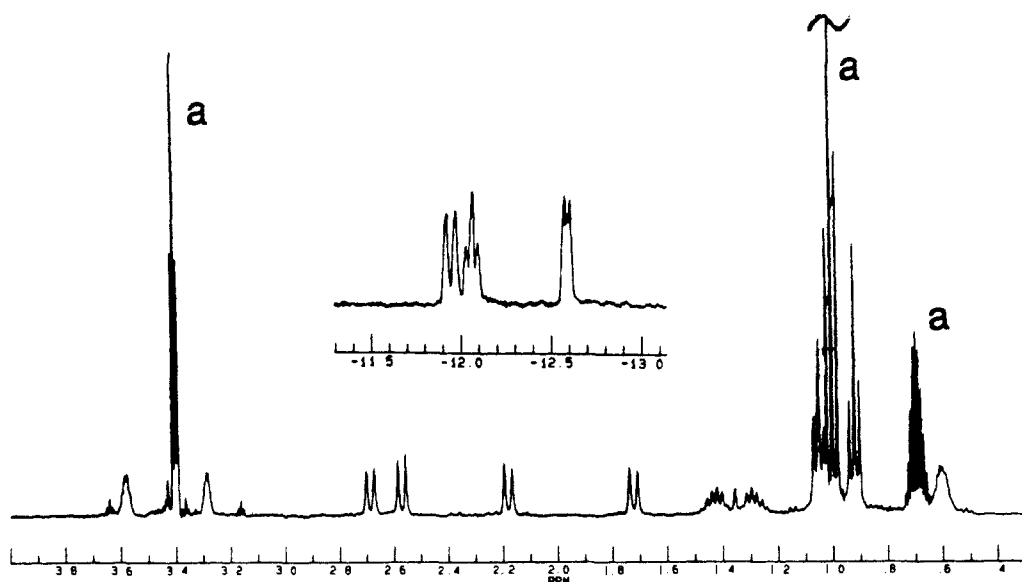


Figure 3. ^1H NMR spectrum of **5b** at -60°C in CD_2Cl_2 . The resonances marked a correspond to dissolved free EtSiH_3 .

($\mu\text{-SiRR}'$) structures.¹⁵ Also notable in the structure of **3a** and **3b** is the diaxial or cis orientation of the R substituents of the $\mu\text{-SiRH}$ ligands.

Characterization of the Dihydride Complex $\text{Rh}_2\text{H}_2(\text{CO})_2(\text{dpam})_2$ (4). Complex **4**, which has not been reported previously, was prepared analogously to **1**. A blue purple solid was obtained from the reaction of a suspension of $\text{Rh}_2\text{Cl}_2(\text{CO})_2(\text{dpam})_2$ with NaBH_4 under H_2 in methanol. The ^1H NMR spectrum of **4** in C_6D_6 displays a triplet at $\delta -10.56$ ppm with coupling to two rhodiums of 15.6 Hz. Compared with **1**, resonances of both $-\text{CH}_2-$ protons and hydrides are sharper due to the absence of coupling to phosphorus. The IR spectrum of **4** shows only one ν_{CO} at 1930 cm^{-1} for the carbonyl ligands, which is consistent with the symmetric structure proposed previously for the dpam analogue **1**. Complex **4** is unstable in solution and air sensitive even in the solid state, serving to preclude further purification to date.

The Reaction of $\text{Rh}_2\text{H}_2(\text{CO})_2(\text{dpam})_2$ (4) with Primary Silanes. Complex **4** reacts with primary silanes to form ultimately the product complexes $\text{Rh}_2(\mu\text{-SiHR})_2(\text{CO})_2(\text{dpam})_2$ (**6a-c**) which are analogous to **3a-c**. These compounds have been characterized spectroscopically and analytically. The absence of ^{31}P coupling in these arsenic derivatives leads to simplification of some of the resonances observed for **3a-c**. Specifically, methylene resonances of dpam ligands appear as doublets and $\mu\text{-SiRH}$ resonances show only coupling with $\alpha\text{-CH}_2$ protons of the alkyl group. The latter confirms that the second-order pattern of the $\mu\text{-SiRH}$ resonance in **3a-c** arises from phosphorus coupling.

When the reaction of **4** with RSiH_3 is performed at -60°C , an intermediate in the formation of **6a-c** is readily observed. This species, **5a-c**, is closely related to, but differs from, the intermediate **2a-c** discussed above. Figure 3 shows the ^1H NMR spectrum for intermediate **5b** obtained in the reaction with EtSiH_3 . Specifically, three unresolved multiplet resonances at δ 5.30, 3.58, and 3.29 ppm are seen in a 1:1:1 ratio, as are four different $-\text{CH}_2-$ protons at δ 2.64, 2.58, 2.18, and 1.72 ppm for the dpam ligands. In addition, **5b** exhibits two different ethyl groups, one of which contains two different $-\text{CH}_2-$ protons, and three distinct metal hydrides with equal intensity. While this intermediate, **5b**, is very unstable in solution even at -40°C , it does not show fluxionality as does **2**. On the basis of its ^1H NMR data and the fact that the final reaction product is $\text{Rh}_2(\mu\text{-SiEtH})_2(\text{CO})_2(\text{dpam})_2$ (**6b**), the intermediate **5b** is proposed to be $\text{Rh}_2(\mu\text{-SiEtH})(\text{SiEtH}_2\text{-H})_3(\text{CO})_2(\text{dpam})_2$.

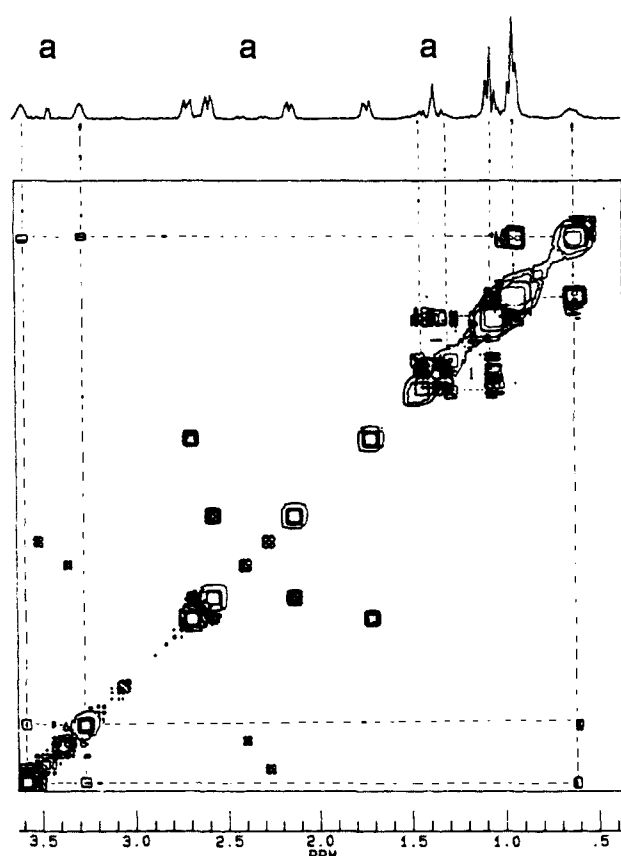


Figure 4. $[\text{H},\text{H}]$ -2D-COSY NMR spectra of **5b** at -60°C in CD_2Cl_2 . The resonances marked a correspond to secondary metal complex products.

On the basis of this structure, the resonance at 5.30 ppm, which is close to the chemical shifts of the $\mu\text{-SiRH}$ protons in **2**, **3**, and **6**, is assigned as the bridging silylene proton of $\mu\text{-SiEtH}$. Likewise, the resonances at δ 3.58 and 3.29 ppm, which are close to the chemical shift of free EtSiH_3 , are assigned to the terminally bonded SiEtH_2 silyl protons. These protons are diastereotopic because of the asymmetric rhodium center and they exhibit slightly different chemical shifts.

The identity of the ethyl resonances belonging to $\mu\text{-SiEtH}$ and SiEtH_2 was elucidated with 2D NMR. The $[\text{H},\text{H}]$ -2D COSY NMR of **5b** at -60°C is shown in Figure 4. The ethyl group having diastereotopic methylene resonances belongs to the $\mu\text{-SiEtH}$

(15) (a) Bennett, M. J.; Simpson, K. A. *J. Am. Chem. Soc.* **1971**, *93*, 7156. (b) Crozat, M. M.; Watkins, S. F. *J. Chem. Soc., Dalton Trans.* **1972**, 2512. (c) Cowie, M.; Bennett, M. J. *Inorg. Chem.* **1977**, *16*, 2321. (d) Simon, G. L.; Dahl, L. F. *J. Am. Chem. Soc.* **1973**, *95*, 783.

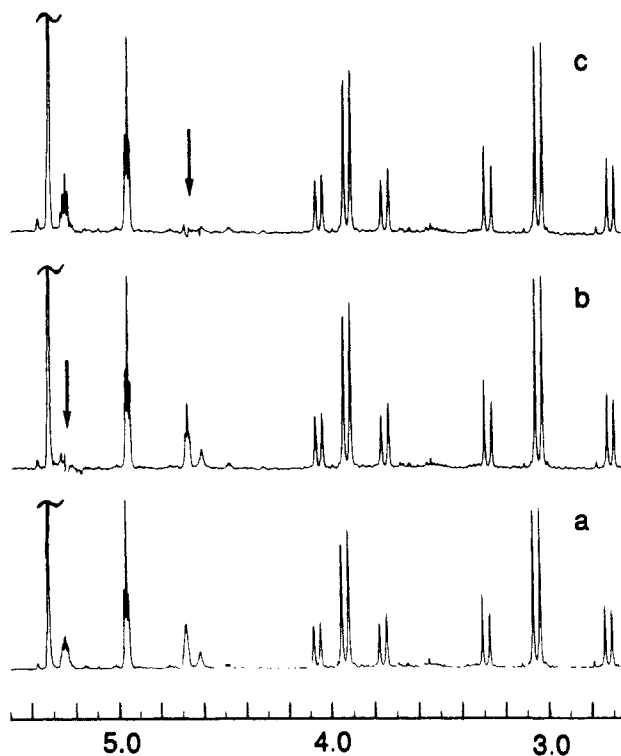


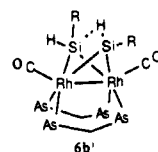
Figure 5. Selective proton decoupling spectra of **6b'** in CD_2Cl_2 at room temperature: (a) without decoupling; (b) decoupling applied on 5.25 ppm; (c) decoupling applied on 4.68 ppm.

ligand as seen through the coupling between $-\text{CH}_3$ and $-\text{CH}_2\text{H}_B$ -resonances. The Et group belonging to the $-\text{SiH}_2\text{Et}$ ligand is identified by the off-diagonal peaks connecting the diastereotopic $\text{Si}-\text{H}$ protons with $-\text{CH}_2-$ of the ethyl group.

Analogous intermediate hydrides **5a** ($\text{R} = \text{Ph}$) and **5c** ($\text{R} = n\text{-C}_6\text{H}_{13}$) are observed in the reaction of **4** with the corresponding primary silane, and both reactions lead to the bis($\mu\text{-SiRH}$) complex $\text{Rh}_2(\mu\text{-SiRH})_2(\text{CO})_2(\text{dpam})_2$ (**6a**, $\text{R} = \text{Ph}$; **6b**, $\text{R} = \text{Et}$; **6c**, $\text{R} = n\text{-C}_6\text{H}_{13}$) as the final product. The product **6a-c** possesses the same kind of cradle-like structure as **3a-c** based on the similarity of ^1H NMR spectra. For **6a**, the $\mu\text{-SiRH}$ resonance is a sharp singlet indicating that the second-order pattern seen for $\mu\text{-SiRH}$ of **3a** is due to coupling to four P donors only. As in the spectra for **3b** and **3c**, **6b** and **6c** exhibit proton-proton coupling between SiRH and the α -methylene protons of the R groups.

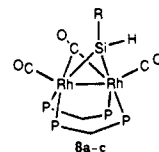
Observation of a Second Product in the Reaction of 4 with EtSiH₃. When the reaction of EtSiH_3 with **4** is carried out in a 2:1 ratio at -60°C with warming to room temperature, an additional product is observed concurrent with the formation of **6b**. After an initial buildup, this product (**6b'**) diminishes, leaving **6b** as the sole product of the reaction. NMR spectroscopy and in particular 2D COSY were used to elucidate the nature of **6b'**. On the basis of these data and the known resonances for the final product **6b**, we find that **6b'** contains two bridging $\mu\text{-SiEtH}$ ligands, no hydrides, and four different methylene resonances of the dpam ligands. The extraordinary feature of **6b'** is the coupling between the two $\text{Si}-\text{H}$ protons even though each SiH proton couples to a different set of $-\text{CH}_2-$ resonances for the two Et groups. Selective decoupling, shown in Figure 5, and 2D COSY were used to show the connection between the two $\text{Si}-\text{H}$ protons. Specifically, when the resonance at δ 5.25 ppm was irradiated, the other $\text{Si}-\text{H}$ resonance at δ 4.68 sharpened and exhibited previously unresolved coupling to the $-\text{CH}_2-$ protons. Likewise, irradiation of the δ 4.68 resonance led to sharpening of the δ 5.25 resonance. From ^1H NMR integration, complex **6b'** appears to be an isomer of **6b**. Although it disappears upon heating, it is stable at -15°C in CD_2Cl_2 for long periods. We propose that **6b'** possesses the cradle structure character of **3** and **6** but with an axial-equatorial interchange of one of the R groups of the $\mu\text{-SiRH}$ ligands. The coupling between $\text{Si}-\text{H}$ resonances arises from a weak

interaction shown by the dotted $\text{H}\cdots\text{Si}$ contact in **6b'** which is approximately trans to the terminal $\text{Si}-\text{H}$ bond.



Analogous chemistry leading to the formation of **6** and **6'** is found with the other primary silanes PhSiH_3 and $n\text{-C}_6\text{H}_{13}\text{SiH}_3$. As in the Et case, **6a'** for $\text{R} = \text{Ph}$ and **6c'** for $\text{R} = \text{C}_6\text{H}_{13}$ is stable in CD_2Cl_2 at -15°C for long periods, but is converted completely to **6** upon warming. If excess RSiH_3 is used in these reactions, product **6'** is unstable and converts readily to the bis($\mu\text{-SiRH}$) product **6**.

Reaction of RSiH_3 with $\text{Rh}_2(\text{CO})_3(\text{dppm})_2$ (7**).** The reaction of **7** with primary silanes proceeds slower than eq 1. In all cases ($\text{R} = \text{Et}, \text{Ph}, n\text{-C}_6\text{H}_{13}$), the reaction proceeds with a rapid color change from dark orange to orange yellow and formation over a period of 1 h at 298 K of a compound, **8**, having a bridging carbonyl and bridging silylene moiety. The $\mu\text{-CO}$ ligand was identified by ν_{CO} at 1770 cm^{-1} while $\mu\text{-SiRH}$ was characterized by the $\text{Si}-\text{H}$ resonance in the region similar to that seen for **3** and **6**. Compound **8a** ($\text{R} = \text{Ph}$) has been isolated analytically pure. Compounds **8a-c** are also observed to form in the reaction of **CO** with intermediates **2a-c** generated in eq 1. On the basis of the spectroscopic and analytical data and the observed reaction chemistry, we formulate **8a-c** as a cradle structure with $\mu\text{-SiRH}$ and $\mu\text{-CO}$ ligands.



When the reaction between $\text{Rh}_2(\text{CO})_3(\text{dppm})_2$ and PhSiH_3 is carried out at low temperature in CD_2Cl_2 , the only observed intermediate on the path to formation of **8a** is the $\mu\text{-SiPhH}$ dihydride **2a**. Since intermediate **2** is seen for up to 15 min in all of the reactions between **7** and RSiH_3 , the formation of **8** is proposed to occur by initial CO loss and RSiH_3 oxidative addition yielding **2** followed by H_2 reductive elimination and CO addition to give the stable product **8**.

The Reactions of 1 with Secondary Silanes. Complex **1** reacts with $\text{RR}'\text{SiH}_2$ substrates leading initially to the formation of $\mu\text{-SiRR}'$ dihydride intermediates $\text{Rh}_2(\mu\text{-SiRR}')(\text{H})_2(\text{CO})_2(\text{dppm})_2$ (**9a**, $\text{R} = \text{R}' = \text{Me}$; **9b**, $\text{R} = \text{R}' = \text{Et}$; **9c**, $\text{R} = \text{Me}, \text{R}' = \text{Ph}$), which are analogous to **2** structurally. The intermediates **9a-c** have been characterized by NMR and IR spectroscopies. The hydride ligand of **9** exhibits a single resonance at room temperature corresponding to a triplet of quintets while the dpmp phosphine donors show themselves as a single second-order pattern for $\text{R} = \text{R}' = \text{Me}$ and **Et** (**9a** and **9b**) and a broad resonance for $\text{R} = \text{Me}, \text{R}' = \text{Ph}$ (**9c**). Upon cooling, the hydride resonance for **9c** first broadens and then sharpens into a second-order pattern similar to that shown in Figure 1, while for **9b** the hydride resonance remains sharp until -60°C , beyond which it broadens. These results indicate that complexes **9a-c** are fluxional, and we propose that exchange occurs between the two hydride ligands of **9** via reductive elimination/oxidative addition steps as in eq 2.

After the reaction of Et_2SiH_2 and **1** has progressed for 24 h at room temperature, a final product is isolated as yellow solid. This product, **10b**, was studied by X-ray diffraction methods and found to have the structure shown in Figure 6. Remarkably, one phenyl group of a dpmp ligand has been cleaved with the formation of a $\text{P}-\text{Si}$ bond. The structure of $\text{Rh}_2(\mu\text{-H})(\text{CO})_2(\text{dppm})\text{-}(\text{Ph}_2\text{PCH}_2\text{PPhSiEt}_2)$ (**10b**) is thus highly distorted and not readily described in terms of either an A-frame or cradle structure. While one dpmp ligand bridges the two rhodium atoms in the expected fashion, the other has undergone $\text{P}-\text{C}(\text{phenyl})$ bond cleavage and

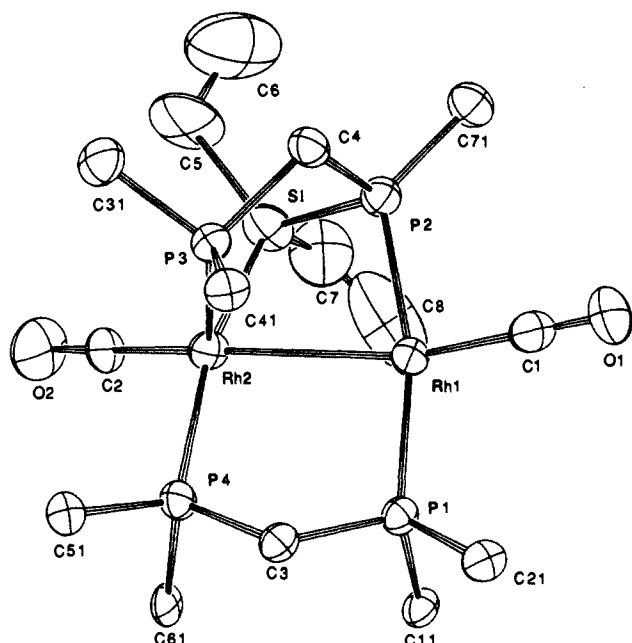


Figure 6. A perspective view of $\text{Rh}_2(\mu\text{-H})(\text{CO})_2(\text{dppm})(\text{Ph}_2\text{PCH}_2\text{PPhSiEt}_2)$ (**10b**). Only the ipso carbon atoms of the phenyl groups are shown for clarity.

Table III. Selected Bond Distances (Å) and Angles (deg) for $\text{Rh}_2(\mu\text{-H})(\text{CO})_2(\text{dppm})(\text{Ph}_2\text{PCH}_2\text{PPhSiEt}_2)$ (**10b**)

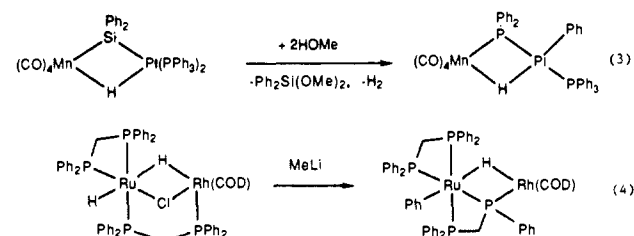
Rh1-Rh2	2.889 (1)	Si-C5	1.91 (2)	Rh1-P2	2.311 (3)
P2-Si	2.244 (4)	P3-C4	1.87 (1)	C1-O1	1.15 (1)
Rh1-P1	2.277 (2)	Rh2-Si	2.347 (3)	Si-C7	1.84 (2)
Rh1-C1	1.83 (1)	Rh2-P3	2.326 (3)	P1-C3	1.82 (1)
Si-Rh2-Rh1	80.56 (9)	Si-Rh2-P3	89.0 (1)		
Si-P2-Rh1	96.9 (1)	Si-Rh2-P4	165.3 (1)		
Si-Rh2-C2	85.4 (3)	P2-Si-Rh2	88.6 (1)		
P2-Si-C5	112.8 (7)	P2-Si-C7	110.8 (7)		
C5-Si-Rh2	118.1 (6)	C7-Si-Rh2	122.2 (7)		
C1-Rh1-Rh2	164.9 (4)	C2-Rh2-Rh1	157.6 (2)		
P1-Rh1-P2	165.1 (1)	P4-Rh2-P3	101.7 (1)		
P2-C4-P3	103.8 (6)	P1-C3-P4	113.6 (5)		
P1-Rh1-Rh2	91.81 (7)	P4-Rh2-Rh1	91.84 (7)		
P2-Rh1-Rh2	75.26 (7)	P3-Rh2-Rh1	77.66 (7)		
O1-C1-Rh1	179 (1)	O2-C2-Rh2	176 (1)		

P-Si bond formation. The SiEt_2 moiety no longer bridges the two rhodium atoms, but instead it is attached to one rhodium and a phosphine bound to the second rhodium. The Rh-Rh bond length is 2.889 (1) Å. While the rhodium bonded to Si has a P-Rh-P angle similar to that of the cradle-like complex **3b**, the other rhodium is coordinated to two nearly trans phosphorus donors with a P-Rh-P angle of 165.1°. Selected bond distances and angles for **10b** are presented in Table III. In addition to the atoms located in the X-ray study, ^1H NMR spectroscopy reveals a broad, highly split resonance attributable to a bridging hydride ligand.

In solution complex **10b** exhibits spectroscopic properties consistent with the structure observed in the solid. In the ^1H and $^{31}\text{P}\{^1\text{H}\}$ NMR spectra, four different methylene protons of the bridging diphosphine ligands and four different phosphorus resonances are seen as expected based on the low symmetry of the structure. The high-field multiplet at -67.52 ppm in the $^{31}\text{P}\{^1\text{H}\}$ NMR spectrum corresponds to the phosphorus bonded to silicon. The hydride multiplet pattern occurs at δ -9.30 ppm in the ^1H NMR spectrum.

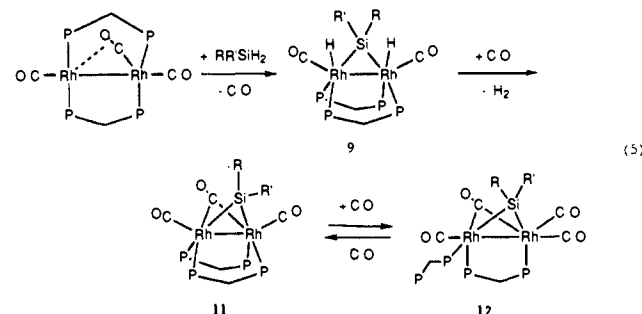
The secondary silanes Me_2SiH_2 and PhMeSiH_2 give analogous final products of formula $\text{Rh}_2(\mu\text{-H})(\text{CO})_2(\text{dppm})(\text{Ph}_2\text{PCH}_2\text{PPhSiRR}')$ (**10a**, $\text{R} = \text{R}' = \text{Me}$; **10b**, $\text{R} = \text{R}' = \text{Et}$; **10c**, $\text{R} = \text{Me}$, $\text{R}' = \text{Ph}$) in which P-C(phenyl) bond cleavage and Si-P bond formation have occurred based on the similarity of their ^1H and $^{31}\text{P}\{^1\text{H}\}$ NMR spectra with those of **10b**.

The cleavage of P-C bonds in transition-metal phosphine complexes is unusual, but by no means unprecedented.¹⁶ This type of cleavage has not been observed previously in the reaction chemistry of the dppm complexes **1** and **7**, and yet the present conditions are exceedingly mild. Comparable examples of P-C cleavage under ambient room temperature conditions include eq 3 reported by Powell¹⁷ and eq 4 reported by Poilblanc.¹⁸ The mechanisms for these transformations are not as yet established. In the present study, the intimate role of the silylene moiety in promoting P-C bond cleavage is unclear.



Compounds with Si-P bonds and organosilylphosphanes in particular have been reviewed by Fritz,¹⁹ but only a few examples are observed involving transition-metal complexes.^{19,20} In these silylphosphine complexes, none shows both Si and P bonded to the transition-metal centers. West has recently described mono- and binuclear complexes based on $\text{Mes}_4\text{Si}_2\text{P}_2$ (Mes = mesityl) which coordinates solely through P lone pairs. In the $\text{Mes}_4\text{Si}_2\text{P}_2$ moiety, the Si atoms are bonded to both P atoms, as well as the Me groups, as seen in the structures of $\text{Pt}(\text{P}_2\text{Si}_2\text{Mes}_4)(\text{PPh}_3)_2$ and $\text{W}_2(\text{CO})_{10}(\mu\text{-P}_2\text{Si}_2\text{Mes}_4)$.²¹

The reaction of Et_2SiH_2 with the tricarbonyl complex **7** is given in eq 5. In comparison with the reaction between primary silanes



and **7**, eq 5 is very slow at ambient temperatures and no products are observed at low temperature. Compound **11b** is formulated as the $\mu\text{-SiEt}_2$ analogue of the $\mu\text{-CO}$ complex **8** based on ^1H and $^{31}\text{P}\{^1\text{H}\}$ NMR and IR spectroscopies. While **11b** is the predominant product of the reaction, it appears to form after initial generation of **9b** as determined by NMR monitoring of the reaction. When the reaction is carried out under CO (200 Torr), another product is observed in high yield which converts to **11b** upon removal of CO. The process is reversible with the new product being generated upon addition of CO to **11b**. On the basis of these observations and the fact that the new product shows four ^{31}P resonances, one of which is a simple doublet far upfield of the other three, we propose this compound to be **12** with a dangling dppm ligand. The resonance of the dangling phosphine resonance is comparable to those of other known complexes containing $\eta^1\text{-dppm}$ ligands.²² Analogous chemistry was found for the

(16) Garrou, P. E. *Chem. Rev.* **1985**, *85*, 171 and references therein.

(17) Powell, J.; Sawyer, J. F.; Shiralian, M. *Organometallics* **1989**, *8*, 577.

(18) Delavause, B.; Chandret, B.; Dahan, F.; Poilblanc, R. *Organometallics* **1985**, *4*, 935.

(19) Fritz, G. *Adv. Inorg. Chem.* **1987**, *31*, 171.

(20) Schafer, H.; MacDiarmid, G. *Inorg. Chem.* **1976**, *15*, 848.

(21) (a) West, R. ACS Central Regional Meeting, John Carroll University, University Heights, Ohio, 1989; Paper 236. (b) Driess, M.; Fanta, A. D.; Powell, D. R.; West, R. *Angew. Chem., Int. Ed. Engl.* **1989**, *28*, 1038.

(22) (a) Bruce, M. I.; Cifuentes, M. P.; Grundy, K. R.; Liddell, M. J.; Snow, M. R.; Tiekink, E. R. T. *Aust. J. Chem.* **1988**, *41*, 603. (b) Brown, M. P.; Yavari, A.; Hill, R. H.; Puddephatt, R. J. *J. Chem. Soc., Dalton Trans.* **1985**, 2421.

reactions of dimethylsilane and methylphenylsilane with **7** leading to the observations of **11a–12a** and **11c–12c**, respectively.

Hydrosilation Reactions. Attempts to use the binuclear complexes **1** and **7** as hydrosilation catalysts were also made. With primary silanes neither complex was active for the hydrosilation of simple olefins or carbonyl compounds, possibly because of the stability of the bis(μ -SiRH) products formed or the reactivity of these systems with primary silanes. However, with secondary silanes modest catalytic activity was found. For ethylene as the substrate, complexes **1** and **7** promote hydrosilation with Me₂SiH₂, Et₂SiH₂, and MePhSiH₂ in benzene at 25 °C at a rate of ~7 turnovers/h while with propylene only catalysis of Me₂SiH₂ hydrosilation could be achieved. The organosilicon products were identified by NMR spectroscopy and GC/mass spectrometry. For carbonyl compounds, hydrosilation reactions yielded silyl enolate products at much slower reaction rates (~0.5 turnovers/h for acetone). The specific carbonyl substrates employed included Me₂CO, MeEtCO, cyclohexanone, and methylcyclopropyl ketone. When large excesses of the silanes were used, the catalytic activity declined sharply.

Conclusions. The present study shows that primary and secondary silanes react rapidly with binuclear dpmm- and dpam-bridged rhodium complexes to form silylene-bridged species. The reactions occur by facile Si–H oxidative addition. For primary silanes, the initially formed μ -SiRH hydrides are fluxional for the dpmm systems with interchange occurring by reversible Si–H oxidative addition/reductive elimination; for the dpam systems, static and more saturated μ -SiRH hydrides are obtained. Subsequent reaction with additional RSiH₃ leads to the formation of stable bis(μ -SiRH) products having cradle structures. For secondary silane substrates, while the initial μ -SiRR' hydrides formed appear strictly analogous to those of the primary silanes, an unusual reaction takes place subsequently which involves P–C(phenyl) cleavage and P–Si bond formation. One of the dpmm ligands is transformed in this reaction into Ph₂PCH₂PPhSiRR', and the resultant complex is highly distorted. The mechanism of this transformation is unclear at the present time. The binuclear dpmm-bridged complexes also catalyze hydrosilation of ethylene and simple carbonyl compounds by secondary silanes, but their effectiveness as catalysts appears limited.

Experimental Section

Physical Measurements. Infrared spectra were recorded on a Mattson Sirius 100 FT-IR spectrometer. ¹H, [¹H, ¹H]-2D-COSY, and ³¹P{¹H} NMR spectra were recorded on a Bruker WH-400 spectrometer at 400 and 162 MHz, respectively. All measurements were carried out at ambient temperature except where noted. Chemical shifts are reported in ppm with residual ¹H in the solvent and external 85% H₃PO₄ as references for ¹H and ³¹P{¹H} NMR, respectively. Mass spectra were measured on a Nermag R10-R10C mass spectrometer with attached gas chromatograph. Microanalyses (C, H) were performed by Desert Analytics Organic Microanalysis, Tucson, AZ.

General Procedures and Reagents. All operations were carried out under vacuum or a N₂ atmosphere with either a high-vacuum line, a modified Schlenk line, or a glovebox. Rhodium trichloride hydrate (Johnson-Matthey), sodium borohydride (J. T. Baker), H₂ (Matheson CP), CO (Gas Products, CP), bis(diphenylarsino)methane (Strem), absolute methanol, bis(diphenylphosphino)methane (Aldrich), and all of the silanes employed (Petrarch Systems) were used as purchased. Methylene chloride, methylene chloride-*d*₂, and benzene-*d*₆ (Aldrich) were dried over CaH₂ for 8 h before use. Benzene and hexane (Aldrich) were dried with sodium benzophenone ketyl and stored under N₂ after vacuum transfer.

Preparation of Complexes. Rh₂H₂(CO)₂(dpmm)₂²³ and Rh₂(CO)₃(dpmm)₂²⁴ were prepared and characterized as described previously. Rh₂Cl₂(CO)₂(dpam)₂ was made by a procedure similar to that used to prepare Rh₂Cl₂(CO)₂(dpmm)₂.²⁵

Rh₂H₂(CO)₂(dpam)₂ (4). Rh₂Cl₂(CO)₂(dpam)₂ (100 mg, 78.3 μmol) and NaBH₄ (50 mg, 1.32 mmol) were placed in a 50-mL flask. Meth-

anol (20 mL) was degassed and syringed into the flask after which the reaction flask was flushed with H₂. The reaction was started at 0 °C and allowed to warm to room temperature slowly. After 1 h, a blue purple solid was isolated and washed with degassed MeOH three times following filtration. The solid was dried under a stream of H₂. ¹H NMR (C₆D₆) 7.64 (s, 16 H), 6.96 (s, 24 H), 3.24 (s, 4 H), –10.56 (t, *J* = 15.6 Hz, 2 H); IR (Nujol) 1930 cm⁻¹.

Rh₂H₂(μ -SiRH)(CO)₂(dpmm)₂ (2, R = Et, Ph). For R = Ph, Rh₂H₂(CO)₂(dpmm)₂ (30 mg, 28.3 μmol) was placed in a 25-mL two-neck flask. Under N₂, PhSiH₃ (6 μL, 42.5 μmol) and CH₂Cl₂ (10 mL) solution were syringed into the flask which was cooled to –30 °C. After 10 min, solvent was partially removed by vacuum, and hexane was added. A yellow-orange solid was isolated and washed with hexane twice after filtration. The product was stored in a glovebox, but decomposed to give Rh₂(CO)₃(dpmm)₂ among other products after several days.

For R = Et, CH₂Cl₂ (10 mL) was transferred into a flask containing 30 mg of Rh₂H₂(CO)₂(dpmm)₂ on a high-vacuum line. The gaseous silane EtSiH₃ (10 mL, 100 Torr) was condensed onto the frozen solution. The reaction was carried out under vacuum at –30 °C for 15 min, and a yellow-orange solid was isolated after hexane was added. For R = *n*-C₆H₁₃SiH₃, the reaction was carried out only in an NMR tube. The relative instability of this series of complexes precluded microanalyses.

2a: ¹H NMR (CD₂Cl₂, –70 °C) 8.29 (d, *J* = 7 Hz, 2 H, Ph), 7.6–6.8 (m, 43 H, Ph), 6.33 (unresolved mult, 1 H, SiH), 4.58 (m, 1 H, CH₂), 4.25 (m, 1 H, CH₂), 2.98 (m, 1 H, CH₂), 2.81 (m, 1 H, CH₂), –9.23 (sym mult, 2 H, Rh–H); ³¹P{¹H} NMR (CD₂Cl₂, –70 °C) 17.9 (syn mult), 28.9 (syn mult); IR (Nujol) ν_{SiH} = 2031 cm⁻¹, ν_{CO} = 1949 cm⁻¹.

2b: ¹H NMR (CD₂Cl₂, –70 °C) 7.4–6.8 (m, 40 H, Ph), 5.94 (unresolved mult, 1 H, SiH), 4.57 (m, 1 H, CH₂), 4.21 (m, 1 H, CH₂), 2.88 (m, 1 H, CH₂), 2.77 (m, 1 H, CH₂), 1.60 (m, 2 H, CH₂), 1.49 (t, *J* = 7 Hz, 3 H, CH₃), –9.48 (sym mult, 2 H, Rh–H); ³¹P{¹H} NMR (CDCl₃, –55 °C) 17.6 (sym mult), 28.98 (sym mult); IR (CD₂Cl₂) ν_{SiH} = 2050 cm⁻¹, ν_{CO} = 1938 cm⁻¹.

2c: ¹H NMR (C₆D₆) 7.62 (s, 8 H, Ph), 7.29 (s, 8 H, Ph), 6.8–6.6 (m, 24 H, Ph), 4.28 (m, 2 H, CH₂), 3.11 (m, 2 H, CH₂), 2.37 (m, 2 H, CH₂), 2.16 (m, 2 H, CH₂), 1.78 (m, 2 H, CH₂), 1.6–1.4 (m, 4 H, CH₂), 1.00 (t, *J* = 8 Hz, 3 H, CH₃), –4.0 (v br); ³¹P{¹H} NMR (CDCl₃, –55 °C) 17.88 (sym mult), 28.62 (sym mult); IR (CD₂Cl₂) ν_{CO} = 1964 cm⁻¹.

Rh₂(μ -SiHR)₂(CO)₂(dpmm)₂ (3). Rh₂H₂(CO)₂(dpmm)₂ (100 mg, 94.4 μmol) was placed in a 50-mL flask and attached to a high-vacuum line. For R = Ph and C₆H₁₃, a solution of RSiH₃ (48 μL, 377.6 μmol) and C₆H₆ (5 mL) was subjected to three freeze–pump–thaw cycles and then transferred into the reaction flask. For R = Et, the gaseous silane was condensed onto the frozen benzene in the reaction vessel. After 24 h of reaction at 60 °C, a white solid was isolated in 40% yield for **3a**. For **3b** and **3c**, the product was isolated in 50–60% yield after hexane was added to the concentrated solution.

3a: ¹H NMR (CD₂Cl₂) 7.78 (m, 8 H, Ph), 7.33 (d, 4 H, Ph), 7.2–6.7 (m, 38 H, Ph), 5.65 (m, 2 H, SiH), 4.68 (m, 2 H, CH₂), 3.22 (m, 2 H, CH₂); ³¹P{¹H} NMR (CD₂Cl₂) 12.50 (sym mult); IR (KBr) ν_{SiH} = 2063 cm⁻¹, ν_{CO} = 1934 cm⁻¹.

3b: ¹H NMR (C₆D₆) 7.87 (s, 8 H, Ph), 7.12 (s, 8 H, Ph), 6.93 (t, *J* = 7 Hz, 10 H, Ph), 6.79 (t, *J* = 7 Hz, 2 H, Ph), 6.65 (t, *J* = 7 Hz, 2 H, Ph), 6.56 (t, *J* = 7 Hz, 10 H, Ph), 5.47 (sym mult, 2 H, SiH), 4.58 (m, 2 H, CH₂), 3.25 (m, 2 H, CH₂), 2.00 (br s, 4 H, SiCH₂), 1.37 (t, *J* = 7 Hz, 6 H, SiCH₂CH₃); ³¹P{¹H} NMR (C₆D₆) 32.61 (sym mult); IR (CH₂Cl₂) ν_{SiH} = 2054 cm⁻¹, ν_{CO} = 1932 cm⁻¹. Anal. Calcd for Rh₂P₄Si₂O₂C₃₆H₅₆: C, 58.6; H, 4.9. Found: C, 57.8; H, 5.1.

3c: ¹H NMR (C₆D₆) 7.88 (s, 8 H), 7.13 (s, 8 H), 6.91 (t, *J* = 7 Hz, 10 H), 6.85 (t, *J* = 7 Hz, 2 H), 6.77 (t, *J* = 7 Hz, 2 H), 6.58 (t, *J* = 7 Hz, 10 H), 5.52 (sym mult, 2 H), 4.59 (m, 2 H), 3.28 (m, 2 H), 2.08 (m, 4 H, SiCH₂), 1.76 (m, 4 H, SiCH₂CH₂), 1.43 (m, 4 H, Si(CH₂)₂CH₂), 1.36 (m, 8 H, Si(CH₂)₃CH₂CH₂), 0.92 (t, *J* = 8 Hz, 6 H, Si(CH₂)₃CH₃); ³¹P{¹H} NMR (C₆D₆) 33.30 (sym mult); IR (CH₂Cl₂) ν_{CO} = 1933 cm⁻¹.

Rh₂(μ -SiHR)₂(CO)₂(dpam)₂ (6). The procedure used to prepare **6** was the same as that used for **3** with the same ratio of reactants (vide supra).

6a: ¹H NMR (C₆D₆) 7.90 (t, *J* = 7 Hz, 12 H), 7.20 (m, 6 H), 7.00 (m, 16 H), 6.80 (q, *J* = 7 Hz, 8 H), 6.60 (t, *J* = 7 Hz, 8 H), 6.29 (s, 2 H), 4.05 (d, *J* = 12 Hz, 2 H), 3.22 (d, *J* = 12 Hz, 2 H); IR (CH₂Cl₂) ν_{CO} = 1943 cm⁻¹, ν_{SiH} = 2032 cm⁻¹. Anal. Calcd for Rh₂As₂Si₂O₂C₆₄H₅₄·2C₆H₆: C, 57.95; H, 4.35. Found: C, 57.48; H, 4.35. The existence of C₆H₆ of crystallization was suggested by the crystal structure of **3a** reported previously^{11a} and was confirmed by the ¹H NMR spectrum of **6a** in CD₂Cl₂.

6b: ¹H NMR (CD₂Cl₂) 7.68 (d, *J* = 8 Hz, 8 H), 7.25 (m, 12 H), 6.99 (m, 12 H), 6.82 (t, *J* = 8 Hz, 8 H), 4.96 (t, *J* = 3 Hz, 2 H), 3.94 (d, *J* = 12 Hz, 2 H), 3.05 (d, *J* = 12 Hz, 2 H), 1.53 (m, 4 H), 0.99 (t, *J* = 8 Hz, 6 H); IR (CH₂Cl₂) ν_{CO} = 1937 cm⁻¹, ν_{SiH} = 2020 cm⁻¹. Anal.

(23) Woodcock, C.; Eisenberg, R. *Inorg. Chem.* **1984**, *23*, 4207.

(24) (a) Kubiak, C. P.; Eisenberg, R. *J. Am. Chem. Soc.* **1980**, *102*, 3637.

(b) Kubiak, C. P.; Woodcock, C.; Eisenberg, R. *Inorg. Chem.* **1982**, *21*, 2119.

(c) Woodcock, C.; Eisenberg, R. *Inorg. Chem.* **1985**, *24*, 1285.

(25) (a) Magure, J. T. *Inorg. Chem.* **1969**, *8*, 1975. (b) Magure, J. T.; Mitchener, J. P. *Ibid.* **1969**, *8*, 119.

Calcd for $\text{Rh}_2\text{As}_4\text{Si}_2\text{O}_2\text{C}_{56}\text{H}_{56}$: C, 50.84; H, 4.27. Found: C, 51.27; H, 4.20.

6c: ^1H NMR (CD_2Cl_2) 7.70 (d, $J = 8$ Hz, 8 H), 7.28 (m, 12 H), 6.98 (m, 12 H), 6.81 (t, $J = 8$ Hz, 8 H), 4.98 (t, $J = 3$ Hz, 2 H), 3.92 (d, $J = 12$ Hz, 2 H), 3.05 (d, $J = 12$ Hz, 2 H), 1.54 (m, 4 H), 1.4–1.2 (m, 16 H), 0.88 (t, $J = 8$ Hz, 6 H); IR (CH_2Cl_2) $\nu_{\text{CO}} = 1933$ cm^{-1} .

$\text{Rh}_2\text{H}_2(\mu\text{-SIRH})(\text{SIRH}_2)(\text{CO})_2(\text{dppam})_2$ (**5**). Complex **5** was only observed at low temperature by ^1H NMR spectroscopy and could not be isolated. The following general procedures were used for the preparation of NMR samples. $\text{Rh}_2\text{H}_2(\text{CO})_2(\text{dppam})_2$ (6 mg, 5.0 μmol) was placed in an NMR tube and attached to a vacuum line. A solution of RSiH_3 (2 μL , 15 μmol ; R = Ph, $n\text{-C}_6\text{H}_{13}$) and 0.5 mL of CD_2Cl_2 was transferred into the NMR tube after 3 freeze–pump–thaw cycles. For R = Et, the gaseous silane was condensed onto the frozen CD_2Cl_2 solution in the NMR tube. The NMR tube was flame sealed and stored at 77 K prior to measurement. The sample was thawed in a dry ice/acetone cooling bath and quickly inserted into the probe (-60 $^\circ\text{C}$) after shaking. Selected ^1H NMR (CD_2Cl_2 , -60 $^\circ\text{C}$) data are given for the complexes.

5a: 5.74 (s, 1 H), 4.14 (s, 1 H), 3.95 (s, 1 H), 2.73 (d, $J = 12$ Hz, 1 H), 2.61 (d, $J = 12$ Hz, 1 H), 2.25 (d, $J = 12$ Hz, 1 H), 1.71 (d, $J = 12$ Hz, 1 H), -11.6 to -11.8 (m, 2 H), -12.40 (m, 1 H).

5b: 5.30 (br s, 1 H), 3.58 (br s, 1 H), 3.29 (br s, 1 H), 2.64 (d, $J = 12$ Hz, 1 H), 2.58 (d, $J = 12$ Hz, 1 H), 2.18 (d, $J = 12$ Hz, 1 H), 1.72 (d, $J = 12$ Hz, 1 H), 1.42 (m, 1 H), 1.28 (m, 1 H), 1.07 (t, $J = 8$ Hz, 3 H), 0.93 (t, $J = 8$ Hz, 3 H), 0.61 (m, 2 H), -11.92 (m, 1 H), -12.05 (m, 1 H), -12.57 (m, 1 H).

5c: 5.24 (br s, 1 H), 3.59 (br s, 1 H), 3.25 (br s, 1 H), 2.64 (d, $J = 12$ Hz, 1 H), 2.58 (d, $J = 12$ Hz, 1 H), 2.09 (d, $J = 12$ Hz, 1 H), 1.72 (d, $J = 12$ Hz, 1 H), -11.92 (m, 1 H), -12.09 (m, 1 H), -12.60 (m, 1 H).

$\text{Rh}_2\text{H}_2(\mu\text{-SIRR}')(\text{CO})_2(\text{dppm})_2$ (**9**). Like **2**, **9** is an air sensitive and thermally unstable intermediate. It was isolated for R = Me, R' = Ph and R = R' = Et by the same procedure as was used for **2a**.

9a: ^1H NMR (C_6D_6) 7.62 (s, 8 H), 7.30 (s, 8 H), 7.0–6.6 (m, 24 H), 3.94 (m, 2 H), 3.02 (m, 2 H), 1.02 (s, 6 H), -8.20 (m, 2 H).

9b: ^1H NMR (C_6D_6) 7.61 (s, 8 H), 7.31 (s, 8 H), 6.9–6.7 (m, 24 H), 3.77 (m, 2 H), 3.06 (m, 2 H), 1.48 (t, $J = 8$ Hz, 6 H), 1.34 (m, 4 H), -8.27 (m, 2 H); ^1H NMR (CD_2Cl_2) 7.42 (s, 8 H), 7.18 (s, 8 H), 7.1–6.9 (m, 24 H), 3.93 (m, 2 H), 2.93 (m, 2 H), 1.09 (t, $J = 8$ Hz, 6 H), 0.90 (q, $J = 8$ Hz, 4 H), -9.15 (trip quint, $J_1 = 24$ Hz, $J_2 = 7$ Hz, 2 H); $^{31}\text{P}\{^1\text{H}\}$ NMR (CD_2Cl_2) 30.00 (sym mult); IR (CH_2Cl_2) 1960 cm^{-1} .

9c: ^1H NMR (CD_2Cl_2 , -70 $^\circ\text{C}$) 8.2 (br s, 2 H), 7.5–6.7 (m, 43 H), 4.54 (m, 1 H), 4.00 (m, 1 H), 3.01 (m, 1 H), 2.79 (m, 1 H), 0.25 (s, 3 H), -9.30 (sym mult, 2 H); $^{31}\text{P}\{^1\text{H}\}$ NMR (CD_2Cl_2 , -70 $^\circ\text{C}$) 29.98 (m), 20.33 (m); IR (Nujol) 1938 cm^{-1} .

$\text{Rh}_2\text{H}(\text{CO})_2(\text{dppm})(\text{Ph}_2\text{PCH}_2\text{PPhSiRR}')$ (**10**). The general procedures used to prepare **10** were similar to those employed for the synthesis of **3**. For Et_2SiH_2 and MePhSiH_2 , a procedure analogous to that for **3a** was utilized. For the gaseous silane Me_2SiH_2 , the procedure for **3b** was employed.

10a: ^1H NMR (C_6D_6) 7.9–7.7 (m, 4 H), 7.6–7.4 (m, 10 H), 7.1–6.5 (m, 21 H), 3.71 (m, 1 H), 3.52 (m, 1 H), 3.23 (m, 1 H), 2.28 (m, 1 H), 1.30 (br s, 3 H), 0.49 (br s, 3 H), -9.40 (m, 1 H); $^{31}\text{P}\{^1\text{H}\}$ NMR (C_6D_6) 33.50 (sym mult), 25.72 (sym mult), 20.12 (sym mult), -65.58 (sym mult); IR (KBr) 1933 cm^{-1} .

10b: ^1H NMR (C_6D_6) 7.85 (t, $J = 8$ Hz, 2 H), 7.77 (t, $J = 8$ Hz, 2 H), 7.6–7.5 (m, 4 H), 7.40 (m, 6 H), 7.1–6.6 (m, 21 H), 3.76 (m, 1 H), 3.59 (m, 1 H), 3.28 (m, 1 H), 2.28 (m, 1 H), 1.6–1.5 (m, 5 H), 0.94 (t, $J = 8$ Hz, 3 H), 0.60 (q, $J = 8$ Hz, 2 H), -9.60 (m, 1 H); $^{31}\text{P}\{^1\text{H}\}$ NMR (C_6D_6) 31.30 (sym mult), 26.00 (sym mult), 19.50 (sym mult), -67.52 (sym mult); IR (CH_2Cl_2) 1952, 1905 cm^{-1} . Anal. Calcd for $\text{Rh}_2\text{P}_4\text{SiO}_2\text{C}_{59}\text{H}_{50}$: C, 57.70; H, 4.84. Found: C, 57.20; H, 4.78.

10c: ^1H NMR (C_6D_6) 8.40 (d, $J = 8$ Hz, 2 H), 7.88 (m, 4 H), 7.6–6.5 (m, 34 H), 3.75 (m, 1 H), 3.60 (m, 1 H), 3.30 (m, 1 H), 2.33 (m, 1 H), 0.82 (s, 3 H) -9.26 (m, 1 H); $^{31}\text{P}\{^1\text{H}\}$ NMR (C_6D_6) 33.50 (sym mult), 26.90 (sym mult), 19.00 (sym mult), -67.50 (sym mult); IR (CH_2Cl_2) 1958, 1910 cm^{-1} .

$\text{Rh}_2(\mu\text{-SIRH})(\mu\text{-CO})(\text{CO})_2(\text{dppm})_2$ (**8**). For R = Ph, $\text{Rh}_2(\text{CO})_3(\text{dppm})_2$ (**7**, 50 mg, 47.2 μmol) was placed in a 25-mL two-neck flask connected to a vacuum line. After the flask was flushed with CO, a solution of PhSiH_3 (56.6 μmol , 10 μL) in benzene (5 mL) was syringed into the flask under CO. The dark orange solution lightened to orange yellow in 5 min and was stirred for 1 h. A yellow solid was obtained upon addition of hexane and was filtered and dried under vacuum. Isolated yield, 75%: ^1H NMR (C_6D_6) 8.48 (d, $J = 7$ Hz, 2 H), 7.90 (m, 4 H), 7.73 (m, 4 H), 7.28 (t, $J = 7$ Hz, 2 H), 7.09 (m, 8 H), 6.9–6.5 (m, 25 H), 5.31 (tt, $J_{\text{PH}} = 23$, 7 Hz, 1 H), 4.20 (dt, $J = 15$, 9 Hz, 1 H), 3.72 (q, $J = 10$ Hz, 1 H), 3.28 (dt, $J = 15$, 9 Hz, 1 H), 2.47 (q, $J = 10$ Hz, 1 H); $^{31}\text{P}\{^1\text{H}\}$ NMR (C_6D_6) 44.86 (sym mult), 24.06 (sym mult); IR (CH_2Cl_2) $\nu_{\text{CO}} = 1946$, 1770 cm^{-1} , $\nu_{\text{SiH}} = 2012$ cm^{-1} . Anal. Calcd for

$\text{Rh}_2\text{P}_4\text{SiO}_3\text{C}_{59}\text{H}_{50}$: C, 60.83; H, 4.33. Found: C, 60.60; H, 4.43.

For R = Et, $\text{Rh}_2(\text{CO})_3(\text{dppm})_2$ (**7**, 50 mg, 47.2 μmol) was dissolved in 5 mL of benzene and frozen. To this solution, EtSiH_3 (10 cc, 150 Torr, 71.4 μmol) was added on a vacuum line followed by the addition of 200 Torr of CO. The reaction was carried out for 1 h with workup similar to that for **8a**. Isolated yield of the yellow solid, 60%: ^1H NMR (C_6D_6) 7.88 (m, 4 H), 7.73 (m, 4 H), 7.1–6.8 (m, 16 H), 6.71 (m, 8 H), 6.60 (t, $J = 7$ Hz, 4 H), 6.54 (t, $J = 7$ Hz, 4 H), 4.65 (br t, $J = 22$ Hz, 1 H), 4.10 (dt, $J = 15$, 9 Hz, 1 H), 3.72 (q, $J = 10$ Hz, 1 H), 3.32 (dt, $J = 15$, 9 Hz, 1 H), 2.44 (q, $J = 10$ Hz, 1 H), 2.07 (m, 2 H), 1.57 (t, $J = 8$ Hz, 3 H); $^{31}\text{P}\{^1\text{H}\}$ NMR (C_6D_6) 45.20 (sym mult), 23.16 (sym mult); IR (CH_2Cl_2) $\nu_{\text{CO}} = 1955$, 1942, and 1768 cm^{-1} .

$\text{Rh}_2(\mu\text{-SiEt}_2)(\mu\text{-CO})(\text{CO})_2(\text{dppm})_2$ (**11b**). $\text{Rh}_2(\text{CO})_3(\text{dppm})_2$ (6 mg, 5.6 μmol) was placed in an NMR tube to which was added a solution of Et_2SiH_2 (3 μL , 20 μmol) in 0.5 mL of C_6D_6 or CD_2Cl_2 after 3 freeze–pump–thaw cycles. The tube was then flame sealed and stored at 77 K before measurement. ^1H NMR (CD_2Cl_2) 7.85 (m, 4 H), 7.48 (s, 4 H), 7.3–6.9 (m, 24 H), 6.83 (m, 4 H), 6.68 (t, $J = 8$ Hz, 4 H), 4.13 (m, 1 H), 3.52 (m, 1 H), 3.35 (m, 1 H), 2.17 (m, 1 H), 1.51 (q, $J = 8$ Hz, 2 H), 1.27 (t, $J = 8$ Hz, 3 H), 0.39 (t, $J = 8$ Hz, 3 H), 0.10 (q, $J = 8$ Hz, 2 H); $^{31}\text{P}\{^1\text{H}\}$ NMR (CD_2Cl_2) 48.00 (sym mult), 28.48 (sym mult); IR (CH_2Cl_2) 1952, 1936, 1770 cm^{-1} .

$\text{Rh}_2(\mu\text{-SiEt}_2)(\mu\text{-CO})(\text{CO})_3(\text{dppm})_2$ (**12b**). A sample similar to that used for **11b** was prepared except under 200 Torr of CO. Following NMR measurements, the sample was opened, solvent was removed, and an infrared spectrum was taken of the isolated precipitate dissolved in CH_2Cl_2 . ^1H NMR (C_6D_6) 7.48 (t, $J = 8$ Hz, 4 H), 7.4–7.2 (m, 8 H), 7.12 (m, 4 H), 6.9–6.7 (m, 24 H), 3.10 (m, 2 H), 2.68 (t, $J = 10$ Hz, 2 H), 1.76 (m, 2 H), 1.65 (m, 2 H), 1.29 (t, $J = 8$ Hz, 6 H); $^{31}\text{P}\{^1\text{H}\}$ NMR (C_6D_6) 25–16 (m, 3 P), -26.80 (d, $J = 40$ Hz, P); IR (CH_2Cl_2) 2001, 1954, 1935, 1768 cm^{-1} .

Hydrosilation of Ketones. A typical reaction was carried out as follows. $\text{Rh}_2(\text{CO})_3(\text{dppm})_2$ (2.8 mg) was dissolved in 0.25 mL of C_6D_6 in an NMR tube. To this solution, acetone (2.0 μL , 27.2 μmol) and methylphenylsilane (2.0 μL , 15.2 μmol) in 0.25 mL of C_6D_6 were added. The NMR tube was flame sealed and the reaction was followed by ^1H NMR spectroscopy after 3.5, 6.5, and 60 h. The ketones used included acetone, cyclohexanone, 2-butanone, and cyclopropyl methyl ketone. The same manipulations were used for the hydrosilation of ethylene with MePhSiH_2 . The reaction was faster than ketone hydrosilation and was followed for shorter periods (10 min, 30 min, 1 h, and 3 h). While **1** appeared to be more reactive than **7** as a catalyst, similar hydrosilation could not be performed because **1** decomposed under the reaction conditions. Blank experiments show that hydrosilation did not occur without **7** even when heated at 60 $^\circ\text{C}$. All organosilicon products were confirmed by ^1H NMR spectroscopy and mass spectrometry.

$\text{CH}_2\text{C}(\text{CH}_3)(\text{OSiMePhH})$: ^1H NMR (C_6D_6) 7.56 (m, 2 H), 7.16 (m, 3 H), 5.35 (q, $J = 2.8$ Hz, 1 H), 4.30 (s, 1 H), 4.08 (s, 1 H), 1.70 (s, 3 H), 0.34 (d, $J = 2.8$ Hz, 3 H); m/e 178.

$\text{CH}_2\text{C}(\text{CH}_2\text{CH}_3)(\text{OSiMePhH})$: ^1H NMR (C_6D_6) 7.61 (m, 2 H), 7.17 (m, 3 H), 5.41 (q, $J = 2.8$ Hz, 1 H), 4.31 (s, 1 H), 4.12 (s, 1 H), 2.07 (q, $J = 10$ Hz, 2 H), 1.00 (t, $J = 10$ Hz, 3 H), 0.38 (d, $J = 2.8$ Hz, 3 H).

$\text{CH}_2\text{CH}_2\text{CH}_2\text{CH}_2\text{CHC}(\text{OSiMePhH})$: ^1H NMR (C_6D_6) 7.65 (m, 2 H), 7.16 (m, 3 H), 5.42 (q, $J = 2.8$ Hz, 1 H), 5.08 (m, 1 H), 2.10 (m, 2 H), 1.88 (m, 2 H), 1.50 (m, 2 H), 1.32 (m, 2 H), 0.34 (d, $J = 2.8$ Hz, 3 H).

$\text{CH}_2\text{C}(\text{CHCH}_2\text{CH}_3)(\text{OSiMePhH})$: ^1H NMR (C_6D_6) 7.56 (m, 2 H), 7.16 (m, 3 H), 5.34 (q, $J = 2.8$ Hz, 1 H), 4.28 (s, 1 H), 4.23 (s, 1 H), 1.33 (m, 1 H), 0.76 (m, 2 H), 0.48 (m, 2 H), 0.34 (d, $J = 2.8$ Hz, 3 H).

EtMePhSiH : ^1H NMR (C_6D_6) 7.45 (m, 2 H), 7.18 (m, 3 H), 4.56 (m, 1 H), 0.94 (t, $J = 8$ Hz, 3 H), 0.72 (m, 2 H), 0.22 (d, $J = 2.8$ Hz, 3 H).

Crystal Structure Determinations. Crystals of **3b** and **10b** suitable for X-ray diffraction analysis were grown from benzene/hexane. The particular crystal of **10b** used for data collection was obtained by cleavage of a larger crystal. Crystallographic data, experimental details of data collection, and structure refinement parameters for both crystal structures are presented in Table I and in Table S1 of the Supplementary Material. The intensity data for structure **3b** showed no evidence of decay upon X-ray irradiation, but the intensity standards for **10b** decayed uniformly by -15.9% and its data set was adjusted by a linear decay correction. Both structures were solved by standard heavy-atom methods with all remaining non-hydrogen atoms located through a succession of difference Fourier maps and least-squares refinements. In the final models for both structure determinations, all heavy atoms were refined anisotropically with hydrogen atoms placed at calculated positions. The final structure of **10b** included a molecule of benzene as a solvent of crystallization which appeared to have an occupancy of ca. 0.5. The thermal ellipsoids for the ethyl carbons of **10b** are relatively large but all distances and

angles regarding those atoms appear within regularly accepted limits.

Acknowledgment. We thank the National Science Foundation (CHE 86-03055 and 89-09060) for support of this work, the Johnson Matthey Co., Inc. for a generous loan of rhodium salts, and Prof. T. Don Tilley of UCSD for communicating results to us prior to publication.

Supplementary Material Available: Tables of refined positional parameters, anisotropic thermal parameters, calculated hydrogen positional parameters, and complete bond distances and angles for non-hydrogen atoms for **3b** and **10b** (18 pages); listing of observed and calculated structure factors for **3b** and **10b** (31 pages). Ordering information is given on any current masthead page.

Structure and Reactivity of Organochromium Macrocyces with Iodine by Chain and Electrophilic Mechanisms

Shu Shi, James H. Espenson,* and Andreja Bakac*

Contribution from Ames Laboratory and the Department of Chemistry, Iowa State University, Ames, Iowa 50011. Received July 19, 1989

Abstract: The kinetic studies on the reaction of $[\text{RCr}([\text{15}] \text{aneN}_4)(\text{H}_2\text{O})]^{2+}$, hereafter $\text{RCrL}(\text{H}_2\text{O})^{2+}$ ($\text{R} = \text{CH}_3, \text{C}_2\text{H}_5, 1\text{-C}_3\text{H}_7, 1\text{-C}_4\text{H}_9, 4\text{-BrC}_6\text{H}_4\text{CH}_2$), macrocyces with iodine show that the reactivity changes as a function of the nature of the organic group bound to chromium(III). In the case of primary alkylchromium(III) macrocyces, the reaction proceeds strictly by bimolecular electrophilic substitution. The specific rates are $4.7 \times 10^3 \text{ M}^{-1} \text{ s}^{-1}$ ($\text{R} = \text{CH}_3$), 81 (C_2H_5), 12 ($1\text{-C}_3\text{H}_7$), 8.9 ($1\text{-C}_4\text{H}_9$), and 9.5 ($4\text{-BrC}_6\text{H}_4\text{CH}_2$). In the case of aralkylchromium(III) and secondary alkylchromium(III) macrocyces, however, both the normal electrophilic substitution and an oxidatively induced chain reaction mechanism are operative. Details of the chain reaction for $\text{R} = \text{BrC}_6\text{H}_4\text{CH}_2$ are reported. The rate constant for the formation of $4\text{-BrC}_6\text{H}_4\text{CH}_2\text{CrL}(\text{H}_2\text{O})^{2+}$ from $\text{CrL}(\text{H}_2\text{O})^{2+}$ and $4\text{-BrC}_6\text{H}_4\text{CH}_2\text{Br}$ was also determined, $k = 3.7 \times 10^4 \text{ M}^{-1} \text{ s}^{-1}$. The crystal and molecular structure of $[4\text{-BrC}_6\text{H}_4\text{CH}_2\text{CrL}(\text{H}_2\text{O})]^{2+}(\text{ClO}_4)_2 \cdot \text{THF}$ was determined. The molecule crystallizes in the space group $P2_1/c$. Cell parameters are $a = 11.683$ (3) Å, $b = 8.816$ (3) Å, $c = 29.959$ (8) Å, and $\beta = 96.29$ (11)°. The chromium is octahedrally coordinated by four N atoms of the macrocyclic ligand at the equatorial positions and by the $4\text{-BrC}_6\text{H}_4\text{CH}_2$ and a water molecule at the axial positions.

The cleavage of metal-carbon bonds by halogens has been fairly widely studied.¹ Generally, two mechanisms are operative. One is electrophilic substitution, often an $\text{S}_{\text{E}2}$ process, that cleanly converts reactants to products. This is usually accompanied by inversion of stereochemistry at the α -carbon atom if the substrate is a transition-metal complex with a high coordination number. The $\text{S}_{\text{E}2}$ mechanism is a two-electron process that occurs without the intervention of reaction intermediates. The second mechanism is a one-electron-transfer process, in which the initial step is the formation of a caged radical pair ($\text{RM}^\cdot, \text{X}_2^\cdot$). The electron-transfer step may initiate a chain sequence for halogenolysis.

The literature in the field includes extensive studies on a series of organochromium complexes, $(\text{H}_2\text{O})_5\text{CrR}^{2+}$,² and macrocyclic complexes of cobalt, including the cobaloximes, $\text{RCo}(\text{dmgH})_2\text{B}$ ($\text{B} = \text{H}_2\text{O}$, pyridine, etc.).³⁻⁶ The former complexes adopt an $\text{S}_{\text{E}2}$ mechanism for halogenolysis, whereas the mechanism for the cobaloximes includes an electron-transfer step. The participation

of inorganic transition-metal complexes in photoinduced chain reactions was also noticed before.⁷

We have turned our attention to iodinolysis reactions of a different group of organometallic complexes. This is a series of alkyl and aralkyl derivatives of a chromium macrocycle, $\text{RCr}([\text{15}] \text{aneN}_4)\text{H}_2\text{O}^{2+}$.⁸ Cleavage of the carbon-chromium bond in such complexes by electrophilic mercury(II) ions occurs strictly by an $\text{S}_{\text{E}2}$ mechanism.⁹ Halogenolysis reactions have not been previously investigated for these complexes. Rather to our surprise, we find that the mechanism for the reaction of $\text{RCr}([\text{15}] \text{aneN}_4)\text{H}_2\text{O}^{2+}$ with I_2 changes along the series of R groups and both electrophilic and oxidative mechanisms have to be considered. We present the results of kinetic investigations in this paper.

No crystal structure data were available for the complexes $\text{RCr}([\text{15}] \text{aneN}_4)\text{H}_2\text{O}^{2+}$ until now. In this work we have determined by X-ray diffraction the structure of the perchlorate salt of the complex with $\text{R} = 4\text{-bromobenzyl}$. Among other factors, we were interested in establishing the identity of the compound on more secure grounds, in the extent of steric hindrance at the chromium-carbon bond, and in the ground-state steric influence, as measured by the extent of the elongation of the bond to the trans water molecule.

Experimental Section

Materials. The chromium(II) complex, CrL^{2+} ($\text{L} = [\text{15}] \text{aneN}_4$), was prepared by mixing stoichiometric amounts of $\text{CrCl}_2 \cdot 4\text{H}_2\text{O}$ ¹⁰ and ligand L (Strem Chemical Co.) in aqueous solution.⁸ The organochromium

(1) Kochi, J. K. *Organometallic Mechanisms and Catalysis*; Academic Press: New York, 1978; Chapter 18.

(2) (a) Espenson, J. H.; Williams, D. A. *J. Am. Chem. Soc.* **1974**, *96*, 1008. (b) Chang, J. C.; Espenson, J. H. *J. Chem. Soc., Chem. Commun.* **1974**, 233. (c) Espenson, J. H.; Samuels, G. J. *J. Organomet. Chem.* **1976**, *113*, 143.

(3) (a) Halpern, J.; Topich, J.; Zamarayev, K. I. *Inorg. Chim. Acta* **1976**, *20*, L21. (b) Topich, J.; Halpern, J. *Inorg. Chem.* **1979**, *18*, 1339.

(4) (a) Dreos, R.; Tauzher, G.; Marsich, N.; Costa, G. *J. Organomet. Chem.* **1975**, *92*, 227. (b) Dreos-Garlatti, R.; Tauzher, G.; Costa, G. *J. Organomet. Chem.* **1977**, *139*, 179. (c) Dreos-Garlatti, R.; Tauzher, G.; Costa, G. *J. Organomet. Chem.* **1979**, *182*, 409.

(5) (a) Okamoto, T.; Goto, M.; Oka, S. *Inorg. Chem.* **1981**, *20*, 899. (b) Fukuzumi, S.; Ishikawa, K.; Tanaka, T. *Chem. Lett.* **1986**, 1801. (c) Fanchiang, Y.-T. *Organometallics* **1985**, *4*, 1515. (d) Fukuzumi, S.; Goto, T.; Ishikawa, K.; Tanaka, T. *J. Chem. Soc., Chem. Commun.* **1989**, 260.

(6) Toscano, P. J.; Barren, E.; Seligson, A. L. *Organometallics* **1989**, in press.

(7) Fukuzumi, S.; Nishizawa, N.; Tanaka, T. *Bull. Chem. Soc. Jpn.* **1983**, *56*, 709.

(8) Samuels, G. J.; Espenson, J. H. *Inorg. Chem.* **1979**, *18*, 2587. $[\text{15}] \text{aneN}_4 = 1,4,8,12\text{-tetraazacyclopentadecane}$.

(9) Samuels, G. J.; Espenson, J. H. *Inorg. Chem.* **1980**, *19*, 233.

(10) Holah, D. G.; Fackler, J. P., Jr. *Inorg. Synth.* **1969**, *10*, 26.